Photocurrent enhancement from an active hybrid TiO_2 film electrode fabricated by a sol–gel method: photocurrent generation during the photooxidation of 4-nonylphenol and 4-nonylphenol polyethoxylate on TiO_2/OTE electrodes

Satoshi Horikoshi,[a] Natsuko Watanabe,[a] Hisao Hidaka*[a] and Nick Serpone[b]

[a] *Frontier Research Center for the Global Environment Protection (EPFC), Meisei University, 2-1-1 Hodokubo, Hino, Tokyo 191-8506, Japan. E-mail: hidaka@epfc.meisei-u.ac.jp*
[b] *Department of Chemistry and Biochemistry, Concordia University, 1455 de Maisonneuve Blvd. West, Montréal (Quebec), Canada H3G-1M8*

Received (in Montpellier, France) 4th March 2002, Accepted 27th May 2002
First published as an Advance Article on the web 12th August 2002

Photocurrent is generated during the photooxidation of nonylphenol polyethoxylate surfactants (NPE-*n*; $n = 1$, 5, 7, 9 and 10), precursors of 4-nonylphenol (NP), on illuminated TiO_2/OTE electrodes on which TiO_2 semiconductor particles were immobilized by a pasting (PA), a sol–gel (SG), or both techniques (HY). The photooxidative process of NP and NPEs was examined by absorption spectroscopic methods monitoring the cleavage of the benzene ring moiety, and by the evolution of CO_2 gas. The kinetics of photooxidation and the magnitude of the generated photocurrent scaled with the length of the ethoxyl side-chain for NPEs where $n = 0$, 1, 5, 7 and 10. The relative order of adsorption of NPEs on the positive TiO_2 surface was predicted from calculated partial negative point charges of all the C and O atoms in the NPEs using molecular orbital methods. Both photodegradation and photocurrent generation were enhanced for the NPE-9 substrate using the HY TiO_2/OTE electrode compared to the PA and SG electrodes. Although, biodegradation of NPEs yields NP in rivers, no formation of NP was observed during the photooxidation of NPE-9 because of predominant opening of the benzene ring. Photooxidation of NPEs is facilitated under an applied bias of +0.3 V and scales with the number of ethoxylate groups.

Introduction

When illuminated with ultraviolet radiation at wavelengths below 387 nm, TiO_2 semiconductor particles exhibit strong oxidative power through the valence band holes, which degrade organic substances through the intermediacy of $^{\bullet}OH$ radicals (and similar reactive oxygen species). This characteristic of titania is being exploited to construct practical devices for wastewater treatment. A significant consideration in such devices is the need for the organic substrates to diffuse toward the illuminated titania, or to be pre-adsorbed on the particles, not least of which is the need for TiO_2 removal by either membrane filtration or by other suitable equivalent methods.

Nonylphenol ethoxylate systems (NPEs) that are discharged into aquatic ecosystems (*e.g.* rivers) are typically biodegraded through bacterial attack of the ethoxyl moieties to yield hydrophobic intermediates of nonylphenol (NP).[1–3] The latter derivative is a toxic substance (an endocrine disruptor), which tends to persist in nature. Consequently, there is a need for this NP endocrine disruptor to be decomposed in relatively short times.

Thin film technologies of fabricating immobilized TiO_2 electrodes have been reported extensively. Noteworthy are the heat treatment of titanium,[4] the laser deposition[5] and sol–gel techniques,[6,7] and chemical vapor deposition methods (CVD)[8] among others. In an earlier study[9] we examined the immobilization of titania particulates on an OTE support by pasting (PA), sol–gel (SG) and hybrid (HY; PA followed by SG) methods. We also noted that in the case of benzene sulfonate as the test substrate,[9] an important step of enhanced degradation was the adsorption of this organic substrate on the TiO_2 surface, an essential mechanistic component for photocurrent generation and photooxidation.

The present study extends the earlier investigation. We examine (a) the photooxidation of NPE-9 and the photocurrent generated by UV illumination of three types of TiO_2 thin film membranes immobilized on an optically transparent electrode (OTE) plate, (b) the effect of the length of the ethoxyl side-chain constituents on the photooxidation and photocurrent generation, and (c) the relationship between photooxidation and photocurrent generated under an applied bias of +0.3 V.

Experimental

Reagents and TiO_2/OTE electrodes

The 4-nonylphenol polyethoxylate (NPE-*n* with $n = 1$, 5, 7, 9 and 10; C_9H_{19}-C_6H_4-O-$(CH_2CH_2O)n$-H; 0.1 mM) surfactants and nonylphenol (NP; C_9H_{19}-C_6H_4-OH; 0.1 mM) were supplied by Miyoshi Oil & Fat Co. and Lancaster, respectively. The supporting electrolyte was an aqueous NaCl solution (100 mM). Optically transparent glass plates (OTE: SnO_2-coated sodalime glass; neat resistance, 5.6 W cm^{-2}; film thickness of SnO_2, 960 nm; a generous gift from Asahi Glass Co.) were used to prepare TiO_2/OTE electrodes. The active TiO_2 photocatalyst was Degussa (titania, P-25; BET area, 53 m^2 g^{-1}; TEM particle size, 20–30 nm; XRD structures, *ca.* 78% anatase, 22% rutile). The dimensions of the OTE plate were

2×4 cm (8 cm^2); TiO_2 covered a 2×3 cm (6 cm^2) area. The details of the preparation of the various TiO_2/OTE electrodes by the PA, SG, and HY methods were reported earlier.[9]

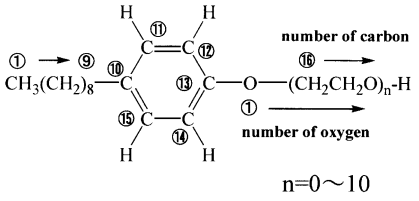

Photoreactive device and analytical measurements

The details of the two-compartment photoreactor used to evaluate the TiO_2/OTE electrodes fabricated by the PA, SG and HY methods to immobilize TiO_2 on the OTE glass plate, together with the operating procedure, were given earlier.[9] In essence, the photoreactor consists of two Pyrex cells which were separated with a glass frit.[10] Aqueous NPEs or NP solutions (0.1 mM, 50 mL) and the supporting electrolyte (NaCl, 100 mM) were contained in this two-compartment photoreactor. The TiO_2/OTE working electrode, the Pt counter-electrode, and the Ag/AgCl reference electrode were all connected to a BAS CV-50 W voltammetric analyzer. The irradiation source was a Toshiba 75-W Hg-lamp, unless otherwise noted. The analyzer was used to control the potential at the TiO_2 surface and to measure the current between the working electrode and the counter-electrode. The UV light was incident on the front side of the TiO_2/OTE plate, which was under an applied anodic bias of +0.3 V (or no applied bias). The light irradiance from this source was 12.5 mW cm^{-2} in the wavelength range 320–400 nm (maximal irradiance, 360 nm).

Some of the characteristic features of the TiO_2 electrodes were given earlier.[9] Scanning electron micrographs (SEM) were taken with a JEOL JSM-5200 electron microscope. The ratio of crystalline type (anatase/rutile ratio) for TiO_2 was obtained with a Rigaku Rad-B X-ray diffractometer (XRD). The contact angles between H_2O, or the NPE-9 solution, and the TiO_2/OTE electrode were assessed with a CA-W150 automatic contact angle meter (Kyowa Interface Science Co. Ltd.). A UV-visible spectrophotometer {JASCO V-570 UV/VIS/NIR} monitored the disappearance of the benzene ring absorption features during the photodegradation of the NPE-9 and NP substrates. The temporal evolution of CO_2 was assayed on a Shimadzu gas chromatograph with TCD detection and equipped with a Porapack Q (CO_2 gas) column; helium was the carrier gas.

Results and discussion

Photodegradation mechanism and photocurrent generation

Photocurrent was generated under 0 V applied bias and under an applied bias of +0.3 V. Conduction band electrons (e^-_{CB}) and valence band holes (h^+_{VB}) in the electrode are produced on titania under UV illumination ($\lambda < 387$ nm; anatase polymorph) of the electrode (reaction 1). The holes are subsequently trapped by HO^- ions on the electrode surface (or by H_2O) to yield $^\bullet OH$ radicals (and H^+; reaction 2). Adsorbed organic pollutants are oxidized by these radicals to give intermediate products and/or are mineralized to carbon dioxide. Our data do not preclude direct oxidation of the substrate (reactions 3 and 4). However, the concentration gradients between water and NPE (or NP) are such that oxidation by $^\bullet OH$ radicals should be the predominant pathway.

$$TiO_2 + h\nu \rightarrow TiO_2(e^-_{CB} + h^+_{VB}) \quad (1)$$

$$h^+_{VB} + (HO^- \text{ and/or } H_2O)_{ads} \rightarrow H^+ + {}^\bullet OH(\text{strong oxidative species}) \quad (2)$$

$$h^+_{VB} + (RH)_{ads} \rightarrow H^+ + R^\bullet \rightarrow\rightarrow (\text{intermediates})_{ads} \quad (3)$$

$$h^+_{VB} + (\text{intermediates})_{ads} \rightarrow H^+ + (\text{intermediates})^\bullet \rightarrow\rightarrow \ldots\ldots\text{mineralized products} \quad (4)$$

The photoproduction of mobile conduction band electrons (e^-) leads to photocurrent generation (process 5) in competition with formation of a small quantity of superoxide radical anions $O_2^{-\bullet}$ (reaction 6) that may also form on the outer surface of the TiO_2 film facing the bulk solution. These $O_2^{-\bullet}$ can interact with protons under acidic conditions to produce $^\bullet OOH$ radicals, also reasonably good oxidizing agents.

$$e^-_{CB} \rightarrow e^-_{OTE} \rightarrow \text{photocurrent} \quad (5)$$

$$e^-_{CB} + (O_2)_{ads} \rightarrow (O_2^{-\bullet})_{ads} \xrightarrow{H^+} {}^\bullet OOH \text{ (oxidative species)} \quad (6)$$

The process(es) occurring at the counter-electrode is (are) depicted in reactions 7 and 8. Reduction of H^+ ions in the (NPEs or NP)-NaCl solution yields $\frac{1}{2}H_2$ at the counter-electrode, and/or HO^- ions by the reduction of water at the Pt electrode. The pH of the solution in the cell with the TiO_2 electrode decreases owing to formation of H^+ ions, whereas the pH of the solution in the cell containing the Pt electrode increases because of formation of OH^- ions and consumption of H^+ ions in reaction 7.

$$H^+ + Pt_{surf} \rightarrow 1/2\ H_2 \quad (7)$$

$$H_2O + Pt_{surf} \rightarrow 1/2\ H_2 + HO^- \quad (8)$$

Characteristics of the three TiO_2/OTE electrodes

The degradation of NPE-9 was monitored by the disappearance of the UV absorption band (222 nm) corresponding to the aromatic component in the NPE-9, as well as by the temporal mineralization of the substrate to CO_2. The photocurrent generated during the photodegradation of NPE-9 on the HY TiO_2 thin film electrode was measured and compared to the photocurrent from the PA and SG electrodes (shown in Fig. 1). Initially, the order of photocurrent generation was SG > HY $\gg$ PA; that continued to *ca.* 100 min of UV irradiation, subsequent to which the order changed to HY > SG $\gg$ PA on further illumination (Fig. 1(a)). The magnitude of photocurrent generated on the PA electrode was relatively low, nearly identical to that observed in the absence of NPE-9 in the H_2O–NaCl control experiment. For the latter, any photocurrent observed with the PA electrode must be due to the photooxidation of water (reaction 2).

The relative disappearance of the UV absorption feature of the benzene ring followed the order HY > SG > PA after 5 h of UV irradiation (Fig. 1(b)). Interestingly, the order is SG > HY > PA for illumination of less than 1 h, remarkably similar to the results obtained in photocurrent generation (note that our data were reproducible to about $\pm$10%). The photomineralization yield in carbon dioxide was 60% when the HY electrode was used, 48% for the SG electrode, and 41% for the PA electrode also after illumination for 5 h. The photodecomposition of NPE-9 occurred on the positively charged TiO_2 surface presumably by initial adsorption through the oxygen atom(s) of one or more of the ethoxyl groups in the side-chain (see the chemical structure in Table 2 below), followed by photooxidative degradation of the ethoxyl side-chain. A possible mechanism for such photooxidations was considered earlier.[11] The total number of carbon atoms in NPE-9 is 33, which consists of 9 alkyl chain carbons (27.3%), 6 benzene ring carbons (18.2%) and 18 carbons for

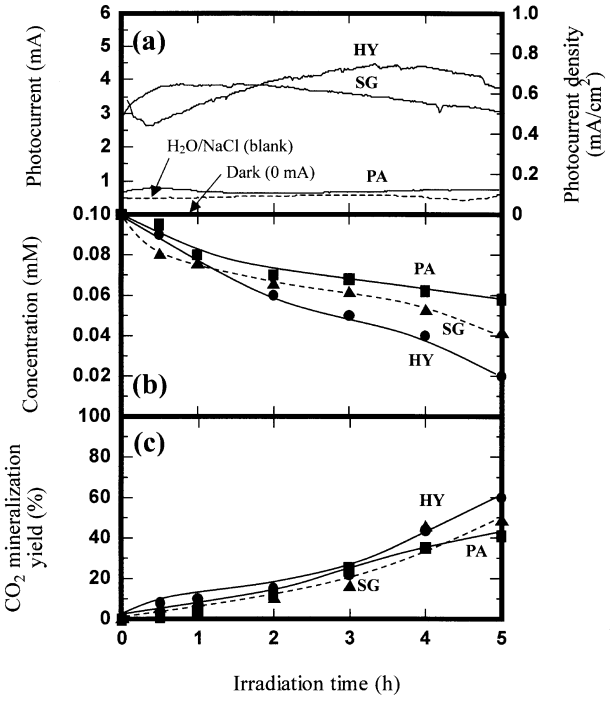

Fig. 1 (a) Temporal generation of photocurrents and current densities, (b) temporal disappearance of the benzene moiety in NPE-9 and (c) temporal photomineralization yields of CO_2 gas in the photodegradation of NPE-9 (0.1 mM, 50 mL) using the PA, the SG, and the HY TiO_2/OTE electrodes under an applied bias of +0.3 V.

the ethoxylate side-chain (54.5%). Since the mineralization yield of CO_2 was 60% from the experimental HY procedure, we deduce that oxidation and cleavage of the benzene ring must have occurred concomitantly with the ethoxyl groups. This is as a result of $^{\bullet}OH$ radical (a strong electrophile) attack on the aromatic ring carbon atoms that possess the larger electron densities (see Table 2 below).

Photooxidations were enhanced on the HY electrode relative to those occurring on the PA or SG electrodes. Evidently, the sol–gel dip-coating procedure to fabricate TiO_2/OTE electrodes from the PA method led to a significant improvement in the photocatalytic features of the HY electrode. The superiority of this HY electrode is likely due to a variety of reasons.

(1) The surface imperfections on the PA electrode, as confirmed by further microscopic magnification,[9] are the result of formation of aggregates by the TiO_2 nanoparticles and of deep crevasses defined by the aggregates. By contrast, the surface of the HY photoelectrode was relatively smooth and flat; the crevasses and imperfections were "annealed" by the sol–gel membrane. The surface characteristics of the HY electrode might be the factor that governs the high retention of TiO_2 particles (Table 1). Weight loss of TiO_2 from a TiO_2/OTE thin film electrode occurred in the degraded solutions when subjected to vigorous agitation for long periods of time. As such, the retention of TiO_2 on TiO_2/OTE electrodes was examined, under otherwise identical conditions, in water (only) under irradiation for 15 h and under vigorous magnetic agitation at 200 rpm; the relevant data are displayed in Table 1. The results show that substantive loss of TiO_2 occurred in the PA electrode (6.5%), none in the SG electrode, and about 1% in the HY electrode.

(2) The crystalline structures of titanium dioxide in the TiO_2/OTE electrodes are also listed in Table 1. The PA procedure did little to the ratio of anatase to rutile in the Degussa P-25 TiO_2 particles immobilized on the OTE glass. The SG method used to prepare titanium dioxide produced 100% anatase. For the HY TiO_2/OTE electrode (SG coating of the PA electrode) the XRD pattern showed a slightly greater quantity of the anatase form (84.3% *versus* 15.7% rutile). This demonstrates that the sol–gel TiO_2 membrane did not completely cover the particles fixed onto the OTE glass by the PA method.[9] The P-25 TiO_2 particles protruding from the HY electrode surface were very photocatalytically active toward degradation of the substrates.

(3) The contact angles between the PA, SG and HY electrodes and a water droplet were 10.3, 39.0 and 17.6°; that is, the affinity of the electrode surface for water varied in the order PA > HY > SG. By contrast, the corresponding contact angles between the electrodes and the NPE-9 solution (see Table 1) show the order of affinity to be HY > PA > SG. (Note that all the contact angle data were obtained under a light irradiance of *ca.* 3 μW cm^{-2}).

Photocurrent generation during the photooxidation of NP and NPEs with different ethoxyl side-chain lengths.

The temporal variations of photocurrent generated and the current densities (mA cm^{-2}) are depicted in Fig. 2. It is evident that the magnitude of the photocurrents depends on the length of the ethoxyl side-chain. In other words, the current density increased with increasing length of the ethoxyl side-chain. The control experiment in which only the electrolyte (NaCl) solution was used (no organic materials) showed that photocurrents are smaller than 0.5 mA, even after irradiation for 5 h. The highest photocurrents were observed during the photodegradation (or direct oxidation) of NPEs and their intermediates on the TiO_2 surface. The initial decrease seen in the first 0.5 h likely reflects the adsorption of the ethoxyl moiety on the TiO_2 electrode surface, subsequent to which the photocurrents increased with further illumination.

Interestingly, the temporal photocurrent generation occurs concomitantly with photodegradation of the NPEs and their intermediate products (see Fig. 2 and 3). Under no bias conditions, the order of the increase in photocurrent was the same as the order observed under the applied bias of +0.3 V; however, some differences were evident. The difference in the applied bias will be relevant to our discussion of the point charge

Table 1 Anatase content (%) of TiO_2 on TiO_2/OTE electrodes from XRD measurements; percent (%) TiO_2 left on TiO_2-fixed OTE electrodes after agitation for 15 h in water only; contact angles between a drop of water or a drop of the NPE-9 solution (0.1 mM) and the TiO_2/OTE electrode surfaces

	PA method	SG method	HY method	SnO_2/glass
% anatase[a]	77.8	100	84.3	—
% retention[b]	93.5	~100	98.8	—
Contact angles with H_2O/°	10.3	39.0	17.6	101
Contact angles with NPE-9/°	20.9	54.3	10.2	75.7

[a] Percent anatase = $100/\{1 + 1.265(I_{rutile}/I_{anatase})\}$; I_{rutile}, $2\theta = 27.42$ degrees; $I_{anatase}$, $2\theta = 25.28$ degrees]. [b] Percent retention = 100 – {(weight after 15 h-stirring)/(initial weight)} × 100.

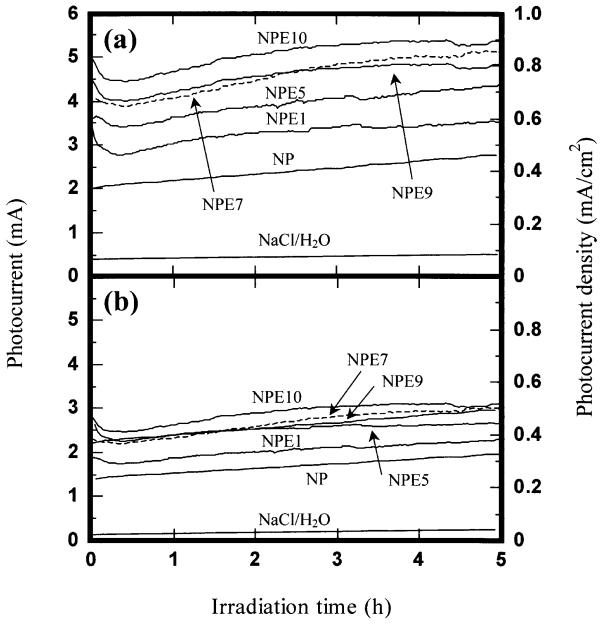

Fig. 2 Temporal evolution of photocurrents and current densities during the photodegradation of NPE-10, -9, -7, -5, -1 and NP (0.1 mM, 50 mL) using the HY TiO_2/OTE electrodes under an applied bias of (a) +0.3 V and (b) under no bias (0 V).

calculations of all the relevant carbon and oxygen atoms in the NPE-*n* ($n = 0, 1, 5, 7, 9,$ and 10) molecules (*e.g.*, see Table 2).

The frontier electron densities and point charges in these NPE-*n* substrates were obtained by MOPAC 97 calculations at the AM1 level available in the CAChe package (see ref. 12–14). These calculations reveal that the largest electron densities on the carbon atoms occur on C10 followed by C13; these are the carbons bonded to the nonyl hydrocarbon residue and to the ethoxyl side-chain, respectively. As a result, these carbon atoms will likely be the prime target for attack by the electrophilic $^{\bullet}OH$ radicals. By contrast the O1 oxygen atom bears the largest electron density among the oxygens, but is approximately four times smaller than those on the carbons.

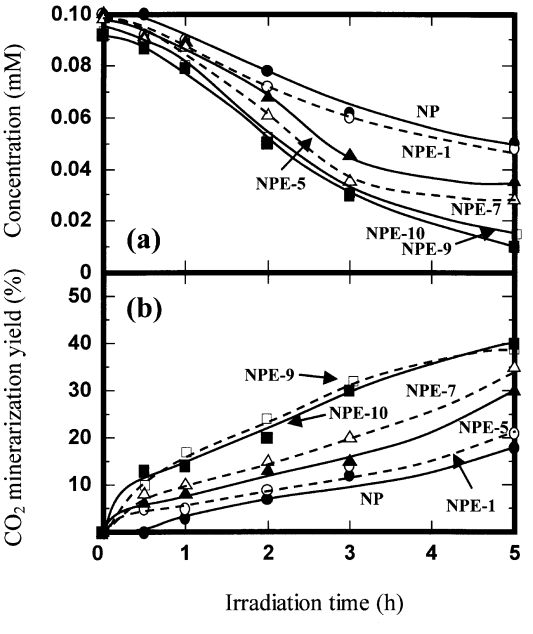

Fig. 3 (a) Temporal degradation of NPE-*n* (benzene ring cleavage), and (b) mineralization yields of CO_2 evolution during the photooxidation of NPEs using the HY TiO_2/OTE electrode under the applied bias of +0.3 V.

To the extent that the TiO_2/OTE electrode surface is positively charged, and that adsorption is mostly a coulombic interaction between this positive surface and the most (partially) negatively charged atoms, the MOPAC 97 calculations can predict which atoms in the structure of the NPE-*n* substrates (Table 2) will be involved. The calculated results also demonstrate that the oxygen atoms of the ethoxyl side-chains carry the largest negative charge; thus, we expect that adsorption of NPEs will occur on the electrode surface predominantly through these oxygens. As well, the greater the number of such partially negatively charged oxygen atoms, the stronger will the substrates be adsorbed on the electrode surface. Accordingly, we infer the order for adsorption to be: NPE-10 = NPE-9 > NPE-7 > NPE-5 > NPE-1 > NPE-0 (or NP). Also, it is apparent that the greater the number of oxygen atoms on the ethoxyl moiety, that is the longer the side-chain, the greater should be the adsorption of the NPEs on the TiO_2 surface. This relative order should also mirror the experimental kinetics of degradation and mineralization of the NPEs (compare Fig. 2 and 3), as well as the magnitude of the photocurrents generated.

In aqueous acidic media, the surface charge of the TiO_2 particles is positive. As we noted earlier (reactions 2–4), photooxidation leads to production of H^+ ions rendering the solution more acidic as the reaction progresses (see Experimental section). The applied bias of +0.3 V increases the surface charge of the TiO_2/OTE electrode. Consequently, adsorption of the NPE systems through the more negatively charged oxygen atoms is enhanced with respect to the condition where no bias is applied (*i.e.*, at 0 V). This prediction is consistent with the experimentally measured photocurrents illustrated in Fig. 2, which show that the magnitude of the photocurrent does scale with the number of ethoxyl groups in the NPEs. It is also consistent with the relative order of photodegradation and CO_2 evolution displayed in Fig. 3 for the NPE-*n* systems. These data provide further support for the notion that adsorption is an important step in the overall degradation process.[15]

In accord with the above expectations, the order of ring opening in the NPE and NP substrates using the HY TiO_2/OTE electrode was NPE-10 = NPE-9 > NPE-7 > NPE-5 > NPE-1 > NP. The rates decreased with increasing UV illumination time. The rates of benzene ring opening also scale with the length of the ethoxyl side-chain. In other words, adsorption of NPEs on the TiO_2 surface is enhanced for longer ethoxyl moieties in the NPE structure. This factor enhances, at least partially, the photodegradation of NPEs. The photomineralization yields with respect to the evolution of CO_2 in the photodecomposition also varied in the same order as the decrease in UV absorption (ring opening). Note that the data for the NPE-9 system in Fig. 2 and 3 are slightly different from the data when the HY electrode was used (see Fig. 1). This deviation is caused by the position of the salt bridge. However, all the experiments in Fig. 1 were done under otherwise identical conditions. Results from Fig. 2 and 3 were also carried out under the same conditions. Therefore, comparison of the data in Fig. 1 or in Fig. 2 and 3 can be made.

In acid solutions, the surface of TiO_2 contains Ti-OH_2^+ functions. The ζ-potential for P-25 TiO_2 particles was *ca.* 0 V at pH = 6.2 in the initial solution, whereas the ζ-potential was greater than *ca.* 0.04 V at pH = 2.8 after irradiation for 5 h. Thus, the surface electric potential was somewhat greater than *ca.* 0.34 V. That is, application of the 0.3 V bias to the total electric potential led to higher rates of photooxidation. This is consistent with the notion that the oxygen positions with greater negative point charges enhance adsorption on the more positive TiO_2 surface. Finally, to the extent that photooxidation and ultimately photomineralization do occur on the TiO_2 photocatalyst surface, photocurrents are also enhanced (Fig. 2). Furthermore, the photocurrent generation

Table 2 Frontier electron densities and point charges for NPE-*n* substrates and for the NP molecule (NPE-*n* for $n = 0$) using semi-empirical Molecular Orbital (MO) calculations using MOPAC 97 (AM1 level) in the CAChe package (see Experimental section for a description of the atom number)

	NP-10	NPE-9	NPE-7	NPE-5	NPE-1	NP
C1	0.0003(−0.233)	0.0004(−0.233)	0.0004(−0.233)	0.0004(−0.233)	0.0004(−0.233)	0.0004(−0.233)
C2	0.0007(−0.173)	0.0008(−0.173)	0.0007(−0.172)	0.0008(−0.172)	0.0007(−0.173)	0.0007(−0.173)
C3	0.0008(−0.171)	0.0009(−0.170)	0.0009(−0.172)	0.0009(−0.171)	0.0009(−0.171)	0.0009(−0.171)
C4	0.0008(−0.171)	0.0009(−0.171)	0.0009(−0.170)	0.0009(−0.171)	0.0008(−0.171)	0.0008(−0.171)
C5	0.0008(−0.171)	0.0009(−0.171)	0.0009(−0.171)	0.0010(−0.171)	0.0009(−0.170)	0.0009(−0.171)
C6	0.0008(−0.171)	0.0009(−0.171)	0.0009(−0.170)	0.0012(−0.171)	0.0009(−0.171)	0.0009(−0.171)
C7	0.0009(−0.170)	0.0010(−0.171)	0.0009(−0.171)	0.0015(−0.170)	0.0009(−0.170)	0.0010(−0.170)
C8	0.0014(−0.169)	0.0014(−0.169)	0.0014(−0.167)	0.0039(−0.167)	0.0015(−0.170)	0.0018(−0.168)
C9	0.0255(−0.139)	0.0253(−0.140)	0.0250(−0.140)	0.0235(−0.140)	0.0241(−0.139)	0.0238(−0.139)
C10	0.4049(−0.135)	0.4015(−0.125)	0.3930(−0.125)	0.3899(−0.124)	0.3864(−0.124)	0.3844(−0.125)
C11	0.2455(−0.127)	0.2308(−0.128)	0.2273(−0.128)	0.2239(−0.130)	0.2240(−0.128)	0.2233(−0.128)
C12	0.2484(−0.207)	0.2464(−0.194)	0.2411(−0.194)	0.2428(−0.193)	0.2382(−0.193)	0.2382(−0.193)
C13	0.3699(0.069)	0.3730(0.052)	0.3661(0.053)	0.3645(0.051)	0.3616(0.051)	0.3590(0.052)
C14	0.2644(−0.229)	0.2512(−0.217)	0.2479(−0.217)	0.2426(−0.214)	0.2414(−0.217)	0.2411(−0.217)
C15	0.2397(−0.127)	0.2415(−0.129)	0.2387(−0.129)	0.2376(−0.129)	0.2346(−0.129)	0.2349(−0.130)
C16	0.0038(−0.055)	0.0042(−0.048)	0.0049(−0.049)	0.0041(−0.051)	0.0040(−0.049)	
C17	0.0009(−0.031)	0.0016(−0.042)	0.0018(−0.042)	0.0015(−0.041)	0.0015(−0.041)	
C18	0.0015(−0.044)	0.0015(−0.045)	0.0015(−0.043)	0.0014(−0.044)		
C19	0.0014(−0.043)	0.0014(−0.043)	0.0014(−0.045)	0.0013(−0.044)		
C20	0.0014(−0.042)	0.0014(−0.043)	0.0014(−0.045)	0.0013(−0.044)		
C21	0.0013(−0.044)	0.0014(−0.043)	0.0014(−0.044)	0.0013(−0.043)		
C22	0.0013(−0.044)	0.0014(−0.043)	0.0014(−0.044)	0.0013(−0.044)		
C23	0.0012(−0.043)	0.0014(−0.043)	0.0013(−0.045)	0.0013(−0.043)		
C24	0.0012(−0.048)	0.0013(−0.043)	0.0013(−0.044)	0.0013(−0.044)		
C25	0.0010(−0.034)	0.0013(−0.043)	0.0014(−0.043)	0.0013(−0.043)		
C26	0.0013(−0.043)	0.0014(−0.043)	0.0013(−0.043)			
C27	0.0012(−0.044)	0.0013(−0.043)	0.0013(−0.043)			
C28	0.0012(−0.049)	0.0013(−0.043)	0.0013(−0.044)			
C29	0.0009(−0.034)	0.0013(−0.042)	0.0013(−0.042)			
C30	0.0013(−0.044)	0.0013(−0.044)				
C31	0.0012(−0.045)	0.0013(−0.044)				
C32	0.0010(−0.032)	0.0011(−0.043)				
C33	0.0012(−0.050)	0.0013(−0.043)				
C34	0.0011(−0.048)					
C35	0.0009(−0.034)					
O1	0.1292(−0.339)	0.1342(−0.276)	0.1305(−0.274)	0.1278(−0.275)	0.1265(−0.272)	0.1262(−0.274)
O2	0.0014(−0.433)	0.0035(−0.355)	0.0036(−0.355)	0.0035(−0.355)	0.0034(−0.356)	
O3	0.0035(−0.357)	0.0035(−0.359)	0.0035(−0.354)	0.0034(−0.359)		
O4	0.0034(−0.356)	0.0035(−0.357)	0.0034(−0.357)	0.0034(−0.359)		
O5	0.0034(−0.358)	0.0035(−0.357)	0.0034(−0.356)	0.0034(−0.359)		
O6	0.0015(−0.432)	0.0034(−0.359)	0.0035(−0.356)	0.0034(−0.358)		
O7	0.0015(−0.435)	0.0034(−0.357)	0.0034(−0.358)			
O8	0.0034(−0.360)	0.0034(−0.358)	0.0034(−0.357)			
O9	0.0033(−0.357)	0.0033(−0.358)				
O10	0.0015(−0.434)	0.0033(−0.359)				
O11	0.0014(−0.434)					

*Frontier electron density (point charge)

and the photodegradation of NPE-9 using the TiO_2/OTE electrode produced by the HY method are more suitable than those from the SG and the PA methods. The relatively large quantity of $^{\bullet}OH$ radicals led to a better harmony between NPE-9 and the TiO_2 surface by the HY method and the highest retention ratio of TiO_2 on the OTE electrode.

Acknowledgements

We are grateful to the Japanese Ministry of Education, Science, Sports, and Culture of Japan (Grant-in-Aid for Scientific Research No. 10640569 to HH), and to the Natural Sciences and Engineering Research Council of Canada (Ottawa; Grant No A5443 to NS) for generous support of our work.

References

1 L. Rudling and P. Solyom, *Water Res.*, 1974, **8**, 115.
2 W. Giger, E. Stephanou and C. Schaffer, *Chemosphere*, 1981, **10**, 1253.
3 E. Stephanou and W. Giger, *Environ. Sci. Technol.*, 1982, **16**, 800.
4 Y. Maeda, M. Ichikawa and Y. Kudo, *Chem. Soc. Jpn.*, 1997, **3**, 227.
5 H. Hidaka, K. Ajisaka, S. Horikoshi, T. Oyama, K. Takeuchi, J. Zhao and N. Serpone, *J. Photochem. Photobiol., A: Chem.*, 2001, **138**, 185.
6 I. Moriguchi, H. Maeda, Y. Teraoka and S. Kagawa, *Chem. Mater.*, 1997, **9**, 1050.
7 I. Moriguchi, H. Maeda, Y. Teraoka and S. Kagawa, *J. Am. Chem. Soc.*, 1995, **117**, 1139.
8 G. K. Boschloo, A. Goossens and J. Schoonman, *J. Electrochem. Soc*, 1997, **144**, 1311.
9 S. Horikoshi, Y. Sato, N. Serpone and H. Hidaka, *J. Photochem. Photobiol. A: Chem.*, 2001, **146**, 109.

10 H. Hidaka, Y. Asai, J. Zhao, K. Nohara, N. Serpone and E. Pelizzetti, *J. Phys. Chem.*, 1995, **99**, 8244.
11 S. Horikoshi, N. Watanabe and H. Hidaka, *J. Jpn. Oil Chem. Soc.*, 2000, **49**, 631.
12 S. Horikoshi, N. Serpone, S. Yoshizawa, J. Knowland and H. Hidaka, *J. Photochem. Photobiol., A: Chem.*, 1998, **120**, 63.
13 K. Fukui, T. Yonezawa, C. Nagata and H. Shingu, *J. Chem. Phys.*, 1953, **11**, 1433.
14 S. D. Kahn, C. F. Pau, L. E. Overman and W. J. Hehre, *J. Am. Chem. Soc.*, 1986, **108**, 7381.
15 J. Zhao, T. Wu, K. Wu, K. Oikawa, H. Hidaka and N. Serpone, *Environ. Sci. Technol.*, 1998, **32**, 2394.